HHS Public Access

Author manuscript

Nature. Author manuscript; available in PMC 2014 June 19.

Published in final edited form as:

Nature. 2013 December 19; 504(7480): 451–455. doi:10.1038/nature12726.

Metabolites produced by commensal bacteria promote peripheral regulatory T cell generation

Nicholas Arpaia[1,2], **Clarissa Campbell**[1,2], **Xiying Fan**[1,2], **Stanislav Dikiy**[1,2], **Joris van der Veeken**[1,2], **Paul deRoos**[1,2], **Hui Liu**[3], **Justin R. Cross**[3], **Klaus Pfeffer**[5], **Paul J. Coffer**[1,6], and **Alexander Y. Rudensky**[1,2,*]

[1]Howard Hughes Medical Institute and Ludwig Center at Memorial Sloan-Kettering Cancer Center [2]Immunology Program, Memorial Sloan-Kettering Cancer Center, New York, NY 10065, USA [3]Donald B. and Catherine C. Marron Cell Metabolism Core Laboratory, Memorial Sloan-Kettering Cancer Center, New York, NY 10065, USA [5]Institute of Medical Microbiology and Hospital Hygiene, Heinrich-Heine-University Duesseldorf, Duesseldorf 40225, Germany [6]Department of Cell Biology, University Medical Center Utrecht, 3584 CX Utrecht, The Netherlands

Abstract

Intestinal microbes provide multicellular hosts with nutrients and confer resistance to infection. The delicate balance between pro- and anti-inflammatory mechanisms, essential for gut immune homeostasis, is affected by the composition of the commensal microbial community. Regulatory T (Treg) cells expressing transcription factor Foxp3 play a key role in limiting inflammatory responses in the intestine[1]. Although specific members of the commensal microbial community have been found to potentiate the generation of anti-inflammatory Treg or pro-inflammatory Th17 cells[2-6], the molecular cues driving this process remain elusive. Considering the vital metabolic function afforded by commensal microorganisms, we hypothesized that their metabolic by-products are sensed by cells of the immune system and affect the balance between pro- and anti-inflammatory cells. We found that a short-chain fatty acid (SCFA), butyrate, produced by commensal microorganisms during starch fermentation, facilitated extrathymic generation of Treg cells. A boost in Treg cell numbers upon provision of butyrate was due to potentiation of extrathymic differentiation of Treg cells as the observed phenomenon was dependent upon intronic enhancer CNS1, essential for extrathymic, but dispensable for thymic Treg cell differentiation[1, 7]. In addition to butyrate, *de novo* Treg cell generation in the periphery was potentiated by propionate, another SCFA of microbial origin capable of HDAC inhibition, but not acetate, lacking this activity. Our results suggest that bacterial metabolites mediate communication

Correspondence and requests for materials should be addressed to A.Y.R. (rudenska@mskcc.org).

Supplementary Information is linked to the online version of the paper at www.nature.com/nature.

Author Contributions: N.A., C.C. and X.F. performed experiments and analyzed data, with assistance from P.D. with HPLC, P.J.C. with Foxp3-Ac immunoprecipitation and J.V. with ChIP-qPCR experiments. H.L. and J.R.C. performed LC-MS. N.A., C.C., X.F. and A.Y.R. designed and interpreted experiments. K.P. provided *Gpr109a* mice. N.A. and A.Y.R. wrote the paper.

The authors declare no competing financial interests.

between the commensal microbiota and the immune system, affecting the balance between pro- and anti-inflammatory mechanisms.

We reasoned that if microbial metabolites facilitate generation of extrathymic Treg cells, such products would be found in the feces of specific pathogen-free (SPF) mice with a normal spectrum of commensal microorganisms, but not microbiota-deficient mice treated with broad-spectrum antibiotics (AVNM) or germ-free (GF) mice. Indeed, we found that polar solvent extracts of feces from SPF, but not GF or AVNM-treated mice potentiated induction of Foxp3 upon stimulation of purified peripheral naïve ($CD44^{lo}CD62L^{hi}CD25^{-}$) $CD4^{+}$ T cells by CD3 antibody in the presence of dendritic cells (DCs), IL-2, and TGF-β (Fig. 1a). Among bacterial metabolites we expected to find short-chain fatty acids (SCFA), and evaluated their content in fecal extracts from SPF, GF or AVNM-treated mice and their ability to affect Treg cell generation. Analysis of hydrazine-derivatized SCFA by HPLC showed a sharp reduction in propionate and butyrate in extracts from GF and AVNM-treated vs. SPF animals (Fig.1b). Concentrations of these SCFA in extracts were in a 5 mM range, corresponding to ∼100-125 μMin *in vitro* Foxp3 induction assays (data not shown). Furthermore, purified butyrate, and to a lesser degree isovalerate and propionate, but not acetate, augmented TGF-β-dependent generation of $Foxp3^{+}$ cells *in vitro* **(**Fig. 1c**; data not shown)**. To exclude the possibility that butyrate allowed for expansion of a few contaminating Treg cells in the starting naïve $CD4^{+}$ T cell population, we took advantage of mice lacking an intronic *Foxp3* enhancer CNS1. These mice are selectively impaired in extrathymic Treg cell differentiation while thymic differentiation is intact [1, 7]. Butyrate failed to rescue the impaired Foxp3 induction in naïve $CD4^{+}$ T cells in the absence of CNS1 (Fig. 1d). Consistent with this result, butyrate did not diminish either qualitatively or quantitatively the TGF-β dependence of Foxp3 induction in CNS1-sufficient $CD4^{+}$T cells (data not shown). These data suggested that butyrate promotes extrathymic differentiation of Treg cells.

In order to determine if butyrate is capable of promoting extrathymic Treg cell generation *in vivo*, we administered butyrate in drinking water to AVNM-treated mice, which exhibit a sharp decrease in microbially-derived SCFAs, or untreated control SPF mice. While we detected only very modest changes, if any, in the lymph node and splenic Treg cell subsets in control mice, provision of butyrate to AVNM-treated animals resulted in a robust increase in peripheral, but not thymic or colonic Treg cells (Fig. 2a, b; Supplementary Fig. 1**; data not shown**). This increase was not an indirect consequence of an inflammatory response because non-lymphoid tissue histology and production of Th1, Th2, and Th17 cytokines by $Foxp3^{-}CD4^{+}$ T cells remained unchanged upon butyrate treatment (data not shown; Supplementary Fig. 2). In agreement with the observed CNS1 dependence of *in vitro* Foxp3 induction, provision of butyrate to AVNM-treated CNS1-deficient mice did not increase the proportion or absolute numbers of Treg cells (Fig. 2c**; data not shown**). Thus, the observed butyrate-mediated increase in the Treg cell subset *in vivo* was due to increased extrathymic generation of Treg cells and not due to their increased thymic output[1, 7]. To ensure that butyrate reconstitution did not result in its non-physiologically high levels, we used LC-MS to compare amounts of butyrate in the serum of AVNM-treated mice that received butyrate versus amounts found in control SPF mice. While virtually undetectable in AVNM-treated

CNS1-sufficient and -deficient animals, butyrate provision resulted in serum levels comparable to those found in unperturbed SPF mice that did not receive butyrate (Fig. 2d). Consistent with the aforementioned unchanged colonic Treg cell subset in AVNM-treated mice that received butyrate via drinking water, levels of butyrate in fecal pellets were not reconstituted in these mice, likely due to its uptake in the small intestine or stomach (data not shown). In contrast, delivery of butyrate via enema into the colon of CNS1-sufficient, but not CNS1-deficient mice, led to an increase in the Treg cell subset in the colonic lamina propria (LP) (Fig. 2e). Thus, local provision of butyrate promoted CNS1-dependent extrathymic generation of Treg cells in the colon. Furthermore, feeding mice butyrylated starch, in the absence of antibiotic treatment, increased colonic Treg cell subsets in comparison to a control starch diet (Supplementary Fig. 3)[8]. In addition to increasing Treg cell numbers, restoration of butyrate levels in AVNM-treated animals did not decrease, but instead increased intracellular Foxp3 protein amounts on a per cell basis in both CNS1-sufficient and -deficient mice, suggesting that this bacterial metabolite might also buttress pre-existing Treg cell populations via stabilization of Foxp3 protein expression (Fig. 2f**; data not shown**).

In contrast to butyrate's ability to increase Treg cell generation in the colon only upon local, but not systemic delivery, other SCFA, namely acetate and propionate, were recently shown to promote accumulation of Treg cells in the colon by activating GPR43[9]. These results suggested discrete modes of action of these three SCFAs. To test this idea we administered AVNM-treated CNS1-sufficient and -deficient mice with propionate and acetate in drinking water. Similarly to butyrate, oral provision of propionate increased Treg cell subsets in the spleen in AVNM-treated CNS1-sufficient, but not -deficient animals, suggesting that propionate also promotes *de novo* generation of peripheral Treg cells (Fig. 2g). In contrast, acetate did not increase splenic Treg cell numbers. These results were fully consistent with our *in vitro* Treg cell differentiation studies (Fig. 1c). In the colon, however, both acetate and propionate, but not butyrate promoted accumulation of Treg cells in a CNS1-independent manner (Fig. 2g). These results suggest that butyrate promotes *de novo* generation, but not colonic accumulation of Treg cells, whereas acetate has a diametrically opposite activity and propionate is capable of both.

The observation that butyrate facilitates extrathymic differentiation of Treg cells raised a question as to whether butyrate directly affects T cells or DCs (or both)by enhancing their ability to induce Foxp3 expression. To explore these non-mutually exclusive possibilities, we assessed the effects of butyrate on the ability of T cells and DCs to generate Treg cells *in vitro* (Fig. 3a-d). We found that butyrate increased, albeit modestly (< 1.5-fold), the numbers of $Foxp3^+$cells in DC-free cultures of purified naive $CD4^+$ T cells stimulated by CD3 and CD28 antibody-coated beads and TGF-β (Fig.3c). Like Treg cells isolated from butyrate-treated mice, Treg cells generated in the presence of butyrate *in vitro* expressed not lower, but rather higher amounts of Foxp3 protein on a per-cell basis than those from butyrate-free cultures (Fig. 3d). This effect was not associated with increased Foxp3 mRNA levels (Fig. 3e, f). Instead, it was likely due to increased Foxp3 protein acetylation observed in the presence of butyrate, a known histone deacetylase (HDAC) inhibitor (Fig. 3g). Foxp3 acetylation confers greater stability and enhanced function [10-13]. Furthermore, the

suppressor activity of Treg cells isolated from mice treated with AVNM and butyrate was not attenuated, but was moderately enhanced as compared to mice treated with AVNM alone (Fig. 3h).

Previous *in vitro* studies suggested that a synthetic HDAC inhibitor, trichostatin A (TSA), potentiates Treg cell generation *in vitro* by acting on T cells [14, 15]. Since butyrate can also boost extrathymic Treg cell generation by acting directly on T cells in the absence of DCs (Fig. 3c), we assessed the effect of butyrate on histone modification at the *Foxp3* locus. When naïve $CD4^+$ T cells from *Foxp3*^{GFP} mice were stimulated by CD3 and CD28 antibody-coated beads and TGF-β with or without butyrate for 3 days, a marked 3-fold increase in H3K27-Ac at the *Foxp3* promoter and CNS1 enhancer was observed in $Foxp3^-$cells purified from these cultures (Fig. 3i). In contrast, increases in the H3K27-Ac occupancy in their $Foxp3^+$ counterparts was expectedly minor (∼30%)and inconsequential. Accordingly, Foxp3 mRNA levels were not different in $Foxp3^+$ cells in the presence or absence of butyrate (Fig. 3e,f). Although we cannot discriminate between the contribution of increased acetylation of histone vs. non-histone targets to heightened Foxp3 induction, it is likely facilitated by the increase in H3K27-Ac observed in $Foxp3^-$T cells.

In addition to its direct Treg cell differentiation-promoting effects on $CD4^+$ T cell precursors, butyrate endowed DCs with a superior ability to facilitate Treg cell differentiation. Pretreatment of DCs with butyrate *in vitro* for 6 h followed by its removal markedly enhanced their ability to induce Foxp3 expression in naïve $CD4^+$ T cells stimulated by CD3 antibody and TGF-β in the absence of butyrate (Fig. 3a; Supplementary Fig. 4a, b). The latter treatment had no detrimental effect on DC viability (Supplementary Fig. 4c). The Foxp3 protein expression induced by butyrate-pretreated and control DCs was comparable, in contrast to a T cell-intrinsic effect of butyrate leading to increased amounts of Foxp3 protein in Treg cells in mice treated with AVNM and butyrate (Fig. 3b, Fig. 2f).

We considered butyrate sensing by G protein-coupled receptors (GPR) as a potential mechanism for the increase in extrathymic differentiation of Treg cells[16, 17]. However, pre-treatment of *Gpr109a*$^{+/+}$ and *Gpr109a*$^{-/-}$ DCs with butyrate similarly increased *in vitro* generation of $Foxp3^+$ cells (Supplementary Fig. 5a). Consistent with these results, butyrate-dependent potentiation of Foxp3 induction by DCs remained unchanged upon pretreatment with pertussis toxin (Supplementary Fig. 5b)[18]. Next, we tested HDAC inhibitory activity of butyrate and other SCFAs in DCs using histone H3 acetylation as an indirect readout (Fig. 4a). TSA and valproate, two chemically distinct HDAC inhibitors, and phenylbutyrate, a butyrate derivative with a relatively weak inhibitory activity, were used as controls in these experiments. Relative HDAC inhibitory activity of SCFAs closely correlated with their ability to potentiate the capacity of DCs to induce Treg cell differentiation. DCs briefly exposed to butyrate, TSA, and to a lesser extent propionate, but not acetate, potently induced Foxp3 expression (Fig.4b). Furthermore, microarray analysis showed that butyrate and TSA induced remarkably similar, if not identical, gene expression changes in DCs (Supplementary Fig. 6a) with a systemic repression of LPS response genes including *Il12*, *Il6*, and *Relb* (Supplementary Fig. 6b,c). Interestingly, repression of *Relb*, a major inducer of DC activation, correlated with the level of HDAC-inhibitory activity of butyrate and other SCFAs (Fig. 4c)[19]. Notably, knockdown of RelB in DC promotes their ability to support

Treg cell differentiation[20, 21]. To further ascertain that TSA and butyrate potentiated Treg cell generation through HDAC inhibition and not through distinct independent mechanisms, we treated DCs with the combination of butyrate and optimal amounts of TSA. If butyrate and TSA were to act via independent mechanisms, they should have exhibited synergistic effects on Foxp3 induction. However, if they acted on identical or related targets, i.e. HDACs, additive effects were unlikely. In support of the latter scenario, we found that butyrate was unable to further enhance the ability of TSA to down-regulate *Relb* and promote Foxp3 induction (Fig. 4d; Supplementary Fig. 6d). These results are consistent with the idea that the HDAC inhibitory activity of butyrate as well as propionate contributes to the ability of DCs to facilitate extrathymic Treg cell differentiation.

In conclusion, our studies suggest that butyrate and propionate, produced by commensal microorganisms, increased extrathymic CNS1-dependent differentiation of Treg cells. Our results indicate that metabolic by-products of commensal microorganisms influence the balance between pro- and anti-inflammatory cells and serve as a means of communication between the commensal microbial community and the immune system.

Methods Summary

CNS1KO (*Foxp3*$^{\Delta CNS1}$), *Foxp3*^{GFP}, *Foxp3*$^{Thy1.1}$ and *Foxp3*^{DTR} mice were previously described[7, 22, 23]. Male C57BL/6 (B6) mice were purchased from The Jackson Laboratory. and groups of 5 co-housed mice were randomly assigned to treatment vs. control groups after confirmation that age and weight were in accordance between groups. Male mice were used for all experiments. All strains were maintained in the Sloan-Kettering Institute animal facility in accordance with institutional guidelines. For antibiotic treatment, mice were given 1 g L^{-1} metronidazole (Sigma-Aldrich), 0.5 g L^{-1} vancomycin (Hospira), 1 g L^{-1} ampicillin (Sigma-Aldrich) and 1 g L^{-1} kanamycin (Fisher Scientific) in drinking water (AVNM). For butyrate, acetate and propionate administration, each SCFA was added to AVNM-containing drinking water at 36 mM and pH-adjusted as needed. DCs were expanded *in vivo* by subcutaneous injection of B16 melanoma cells secreting FLT3-ligand and purified using CD11c (N418) magnetic beads (Dynabeads, Invitrogen). *In vitro* Foxp3 induction assays were performed by incubating 5.5 × 10^4 FACS-sorted naïve CD44^{lo}CD62L^{hi}CD25^{-}CD4^{+}T cells with 1 μg ml^{-1} of CD3 antibodyin the presence of DCsin 96-well flat-bottom plates for 4 d. Alternatively, naïve CD4^{+}T cells were stimulated with CD3 and CD28 antibody-coated beads (Dynabeads Mouse T-Activator, Invitrogen) at a 1:1 cell-to-bead ratio. All cultures were supplemented with 1 ng mL^{-1} TGF-β and 100 U ml^{-1} IL-2. Intracellular staining for IL-17, IFN-γ, IL-4, IL-13 and Foxp3 was performed using the Foxp3 staining kit (eBiosciences). Cytokine staining was performed after re-stimulation of *ex vivo* isolated cells with 5 μg ml^{-1} CD3 antibody and 5 μg ml^{-1} CD28 antibody in the presence of Golgi-plug (BD Biosciences) for 5 h. Stool samples were collected directly into sterile tubes from live mice and snap-frozen before preparation of material for SCFA quantification by HPLC or LC-MS. HPLC analysis of 2-nitrophenylhydrazine HCl-derivatized SCFA present in stool extracts was performed as describedelsewhere [24]. H3K27Ac ChIP-qPCR was performed as previously described[25].

Methods

Mice

Foxp3$^{\Delta CNS1}$ (CNS1 knockout), *Foxp3*^{GFP}, *Foxp3*$^{Thy1.1}$ and *Gpr109a*$^{-/-}$ mice have been previously described[7, 22, 23]. Male C57BL/6 (B6) mice were purchased from the Jackson Laboratory and groups of 5 co-housed mice were randomly assigned to treatment vs. control groups after confirmation that age and weight were in accordance between groups. Male mice were used for all experiments. All strains were maintained in the Sloan-Kettering Institute animal facility in accordance with institutional guidelines. Mice were sacrificed by CO_2 asphyxiation then blindly processed for tissue harvest thereafter. For antibiotic treatment, mice at 5-6 weeks of age were treated with 1 g L^{-1} metronidazole (Sigma-Aldrich), 0.5 g L^{-1} vancomycin (Hospira), 1 g L^{-1} ampicillin (Sigma-Aldrich) and 1 g L^{-1} kanamycin (Fisher Scientific) dissolved in drinking water. For butyrate, acetate and propionate administration, each SCFA was added to drinking water containing antibiotics (as described above) at a final concentration of 36 mM and pH-adjusted, if needed, to match that of antibiotic-only water. Butyrate was administered to mice after prior treatment with antibiotics for at least 1 wk.

Cell isolation and FACS staining

For in vitro experiments, $CD4^+$ T cells and $CD11c^+$ dendritic cells were enriched using mouse CD4 (L3T4, Invitrogen) and mouse CD11c (N418, BioLegend) antibodies, respectively, that were biotinylated for use with streptavidin-Dynabeads (Invitrogen). Enriched cells were then sorted on a FACSAria II cell sorter (BD Biosciences) for *in vitro* assays. Intracellular staining for IL-17, IFN-γ, IL-4, IL-13 and Foxp3 was performed using the Foxp3 staining kit (eBiosciences). Cytokine staining was performed after re-stimulation with CD3 antibody and CD28 antibody(5 μg ml^{-1} each) in the presence of Golgi-plug (BD Biosciences) for 5 h.

Dendritic cellgeneration and isolation

DC were expanded *in vivo* by subcutaneous injection of B16 melanoma cells secreting FLT3-ligand into the left hind flank of mice as indicated. Once tumors were visible, spleens from injected animals were dissociated in RPMI 1640 medium containing 1.67 U mL^{-1} liberase TL (Roche) and 50 μg mL^{-1} DNAse I (Roche) for 20 min at 37 °C with shaking. EDTA was then added at a final concentration of 5 mM to stop digestion and the resulting homogenate was processed for $CD11c^+$ cell isolation using the MACS mouse CD11c (N418) purification kit (Miltenyi Biotec).

In vitro assays

In vitro Foxp3 induction assays were performed by co-culturing DC with 5.5×10^4 $CD4^+CD44^{lo}CD62L^{hi}CD25^-$ naïve T cells in the presence of 1 μg ml^{-1} of CD3 antibody, 1 ng mL^{-1} TGF-β, and 100 U ml^{-1} IL-2, in 96-well flat-bottom plates for 4 d. For Foxp3 induction in the presence of butyrate- or TSA-pretreated DC, TGF-β was used at 0.1 ng mL^{-1} final concentration. *In vitro* induction assays in the absence of DC were performed by incubating 5.5×10^4 naïve $CD4^+$ T cells with 1 ng mL^{-1} TGF-β, 100 U ml^{-1} IL-2, and a 1:1

cell-to-bead ratio of CD3/CD28 T activator Dynabeads (Invitrogen). For in vitro suppression assays, 4×10^4 naïve $CD4^+$ T cells were FACS-sorted from B6 mice and cultured with graded numbers of $CD4^+Foxp3^+$ Treg cells FACS-sorted from *Foxp3*^{GFP} mice treated with antibiotics and with or without butyrate, in the presence of 10^5 irradiated T cell-depleted splenocytes and 1 μg ml^{-1} CD3 antibody in a 96-well round-bottom plate for 80 h. Proliferation of T cells was assessed by [^{3}H]-thymidine incorporation during the final 8 h of culture.

Chromatin immunoprecipitation (ChIP)-qPCR assays

H3K27Ac ChIP-qPCR was performed as previously described[25]. Briefly, fixed cells were lysed and mono- and poly-nucleosomes were obtained by partial digestion with micrococcal nuclease (12,000 U mL^{-1}) in 1 min at 37 °C. EDTA was added to a final concentration of 50 mM to stop the reaction, and digested nuclei were resuspended in nuclear lysis buffer with 1% SDS. After sonication, 1 ug H3K27Ac-specific antibody (Abcam, ab4729) was used to precipitate H3K27Ac-bound chromatin. Washing and de-crosslinking was performed as described[25].

Stool sample collection

Stool samples were collected directly into sterile tubes from live mice and snap-frozen before preparation of material for SCFA quantification by HPLC or LC-MS (see corresponding section for further sample processing).

HPLC assays

HPLC analysis was performed for analysis of derivatized stool extracts as previously described[24]. Briefly, flash-frozen stool samples were extracted with 70% ethanol and brought to a final concentration of 0.1 μg μL^{-1}. Debris was removed by centrifugation and 300μL of supernatant was transferred to a new tube and combined with 50 μL of internal standard (2-ethylbutyric acid, 200 mM in 50% aqueous methanol), 300μL of dehydrated pyridine 3% v/v (Wako) in ethanol, 300 μL of 250 mM N-(3-dimethlaminopropyl)-N′;-ethylcarbodiimide hydrochloride (Sigma-Aldrich) in ethanol, and 300 μL of 20 mM 2-nitrophenylhydrazine hydrochloride (Tokyo Chemical) in ethanol. Samples were incubated at 60 °C for 20 min and 200 μL of potassium hydroxide 15% w/v dissolved 80/20 in methanol was added to stop the derivatization reaction. Samples were incubated again at 60 °C for 20 min and transferred into a glass conical tube containing 3 mL of 0.5 M phosphoric acid. The organic phase was extracted by shaking with 4 mL diethyl ether and transferred to a new glass conical containing water to extract any remaining aqueous compounds. The organic phase containing the derivatized SCFA was transferred into a new 5 mL glass vial and evaporated overnight in a fume hood. Derivatized SCFA were resuspended in 100 μL of mobile phase (below) and 20 μL was chromatographed on a Shimadzu HPLC system equipped with a Vydac 2.1 × 30 mm 300 A C18 column run at 200 μL min^{-1} in methanol/acetonitrile/TFA (30%/16%/0.1% v/v) and monitored for absorbance at 400 nm.

LC-MS assays

300 μl 80% methanol containing deuterated short chain fatty acid internal standards (Cambridge Isotope Laboratories) was added to 70 μL serum and incubated at −80 °C for 30 min. Samples were then centrifuged at 4 °C at 14000 rpm for 15 min to precipitate protein. Pure short chain fatty acid standards (Sigma-Aldrich) were also prepared in 300 μl 80% methanol containing internal standards to produce a calibration curve from 0.25 μM to 50 μM. 80% methanol extracts were combined with 300 μl 250 mM N-(3-dimethylaminopropyl)-N′-ethylcarbodiimide hydrochloride in ethanol, 300 μL 20 mM 2-nitrophenylhydrazine hydrochloride in ethanol and 300 μL 3% pyridine in ethanol in a glass tube and reacted at 60°C for 20 min. The reaction was quenched with 200 μL potassium hydroxide solution (15% KOH : MeOH, 8 : 2 v/v) at 60°C for 20 min. After cooling, the mixture was adjusted to pH 4 with 0.25 M HCl. Derivatized short chain fatty acids were then extracted with 4 mL ether and washed with 4 mL water before drying under a nitrogen stream. The dried sample was dissolved in 150 μL methanol, and 5 μL was injected for LC-MS analysis.

Butyrate enemas

Mice were anesthetized with isoflurane and injected intrarectally with 200 μL of 50 mM butyric acid (pH 4.0) or pH-matched water delivered through a 1.2 mm-diameter polyurethane catheter (Access Technologies, Skokie, IL). Enemas were administered for 7 days.

Supplementary Material

Refer to Web version on PubMed Central for supplementary material.

Acknowledgments

This work was supported by the Robert Black Fellowship of the Damon Runyon Cancer Research Foundation DRG-2143-13 (N.A.), Ludwig Center at Memorial Sloan Kettering Cancer Center and National Institutes of Health (NIH) grant T32 A1007621 (N. A.) and R37 AI034206 (A.Y.R.). A.Y. Rudensky is an investigator with the Howard Hughes Medical Institute.

References

1. Josefowicz SZ, et al. Extrathymically generated regulatory T cells control mucosal T(H)2 inflammation. Nature. 2012; 482:395–U1510. [PubMed: 22318520]
2. Round JL, Mazmanian SK. Inducible Foxp (3+) regulatory T-cell development by a commensal bacterium of the intestinal microbiota. Proceedings of the National Academy of Sciences of the United States of America. 2010; 107:12204–12209. [PubMed: 20566854]
3. Ivanov II, et al. Induction of intestinal Th17 cells by segmented filamentous bacteria. Cell. 2009; 13998:485. [PubMed: 19836068]
4. Lathrop SK, et al. Peripheral education of the immune system by colonic commensal microbiota. Nature. 2011; 478:250–4. [PubMed: 21937990]
5. Atarashi K, et al. Induction of Colonic Regulatory T Cells by Indigenous Clostridium Species. Science. 2011; 331:337–341. [PubMed: 21205640]
6. Atarashi K, et al. Treg induction by a rationally selected mixture of Clostridia strains from the human microbiota. Nature. 2013; 500:232–6. [PubMed: 23842501]

7. Zheng Y, et al. Role of conserved non-coding DNA elements in the Foxp3 gene in regulatory T-cell fate. Nature. 2010; 463:808–12. [PubMed: 20072126]
8. Annison G, Illman RJ, Topping DL. Acetylated, propionylated or butyrylated starches raise large bowel short-chain fatty acids preferentially when fed to rats. J Nutr. 2003; 133:3523–8. [PubMed: 14608068]
9. Smith PM, et al. The microbial metabolites, short-chain fatty acids, regulate colonic Treg cell homeostasis. Science. 2013; 341:569–73. [PubMed: 23828891]
10. van Loosdregt J, et al. Rapid temporal control of Foxp3 protein degradation by sirtuin-1. PLoS One. 2011; 6:e19047. [PubMed: 21533107]
11. van Loosdregt J, et al. Regulation of Treg functionality by acetylation-mediated Foxp3 protein stabilization. Blood. 2010; 115:965–74. [PubMed: 19996091]
12. Zhang H, Xiao Y, Zhu Z, Li B, Greene MI. Immune regulation by histone deacetylases: a focus on the alteration of FOXP3 activity. Immunol Cell Biol. 2012; 90:95–100. [PubMed: 22124370]
13. Song X, et al. Structural and biological features of FOXP3 dimerization relevant to regulatory T cell function. Cell Rep. 2012; 1:665–75. [PubMed: 22813742]
14. Wang L, de Zoeten EF, Greene MI, Hancock WW. Immunomodulatory effects of deacetylase inhibitors: therapeutic targeting of FOXP3+ regulatory T cells. Nat Rev Drug Discov. 2009; 8:969–81. [PubMed: 19855427]
15. Tao R, et al. Deacetylase inhibition promotes the generation and function of regulatory T cells. Nat Med. 2007; 13:1299–307. [PubMed: 17922010]
16. Maslowski KM, et al. Regulation of inflammatory responses by gut microbiota and chemoattractant receptor GPR43. Nature. 2009; 461:1282–U119. [PubMed: 19865172]
17. Thangaraju M, et al. GPR109A is a G-protein-coupled receptor for the bacterial fermentation product butyrate and functions as a tumor suppressor in colon. Cancer Res. 2009; 69:2826–32. [PubMed: 19276343]
18. Nilsson NE, Kotarsky K, Owman C, Olde B. Identification of a free fatty acid receptor, FFA2R, expressed on leukocytes and activated by short-chain fatty acids. Biochem Biophys Res Commun. 2003; 303:1047–52. [PubMed: 12684041]
19. MacDonald KP, et al. Effector and regulatory T-cell function is differentially regulated by RelB within antigen-presenting cells during GVHD. Blood. 2007; 109:5049–57. [PubMed: 17327399]
20. Zhu HC, et al. Tolerogenic dendritic cells generated by RelB silencing using shRNA prevent acute rejection. Cell Immunol. 2012; 274:12–8. [PubMed: 22464914]
21. Shih VF, et al. Control of RelB during dendritic cell activation integrates canonical and noncanonical NF-kappaB pathways. Nat Immunol. 2012; 13:1162–70. [PubMed: 23086447]
22. Fontenot JD, et al. Regulatory T cell lineage specification by the forkhead transcription factor foxp3. Immunity. 2005; 22:329–41. [PubMed: 15780990]
23. Kim JM, Rasmussen JP, Rudensky AY. Regulatory T cells prevent catastrophic autoimmunity throughout the lifespan of mice. Nat Immunol. 2007; 8:191–7. [PubMed: 17136045]
24. Torii T, et al. Measurement of short-chain fatty acids in human faeces using high-performance liquid chromatography: specimen stability. Annals of Clinical Biochemistry. 2010; 47:447–452. [PubMed: 20595408]
25. Samstein RM, et al. Foxp3 exploits a pre-existent enhancer landscape for regulatory T cell lineage specification. Cell. 2012; 151:153–66. [PubMed: 23021222]

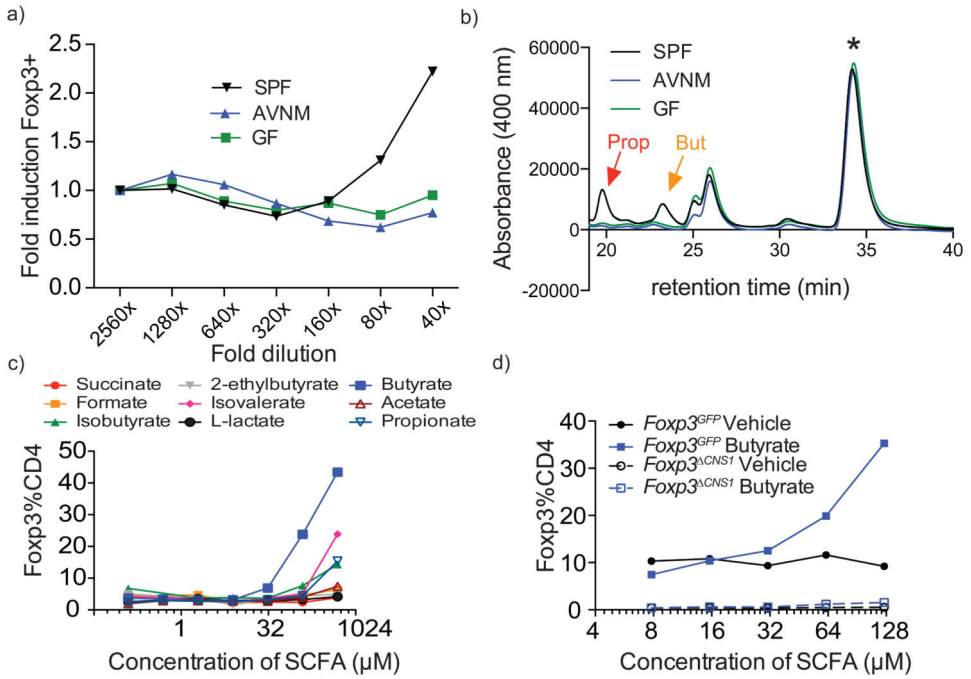

Figure 1. SCFA produced by commensal bacteria stimulate *in vitro* generation of Treg cells

a) Effect of fecal extracts from SPF, antibiotic-treated (AVNM), or germ-free (GF) mice on *in vitro* induction of Foxp3 expression in naïve $CD4^+$ T cells stimulated with CD3 antibody in the presence of Flt3L-elicited DC and TGF-β. Foxp3 expression was assessed by flow cytometric analysis on day 4 of culture. Naïve $CD25^+CD62L^{hi}CD44^{lo}CD4^+$ T cells were FACS-purified from B6 mice. Fecal extracts were prepared in 70% ethanol. Data are shown as fold induction over corresponding dilution of vehicle and are representative of 2 independent experiments.

b) HPLC fractionation of 2-nitrophenylhydrazine-HCl derivatized SCFA present in indicated fecal extracts. Red and yellow arrows indicate peaks corresponding to propionate and butyrate, respectively. Internal standard peak is indicated with a star. The HPLC fractionation profile of fecal extracts pooled from three animals each is representative of two independent experiments.

c) Effect of indicated purified SCFA on *in vitro* induction of Foxp3 expression in naïve $CD4^+$ T cells isolated from B6 or *Foxp3*^{GFP} mice as described in (a). Data are representative of 3 independent experiments.

d) Effect of butyrate on Foxp3 induction in CNS1-sufficient and -deficient naïve $CD4^+$ T cells from *Foxp3*^{GFP} and *Foxp3*$^{\Delta CNS1}$ as described in (a). Data are representative of at least two independent experiments.

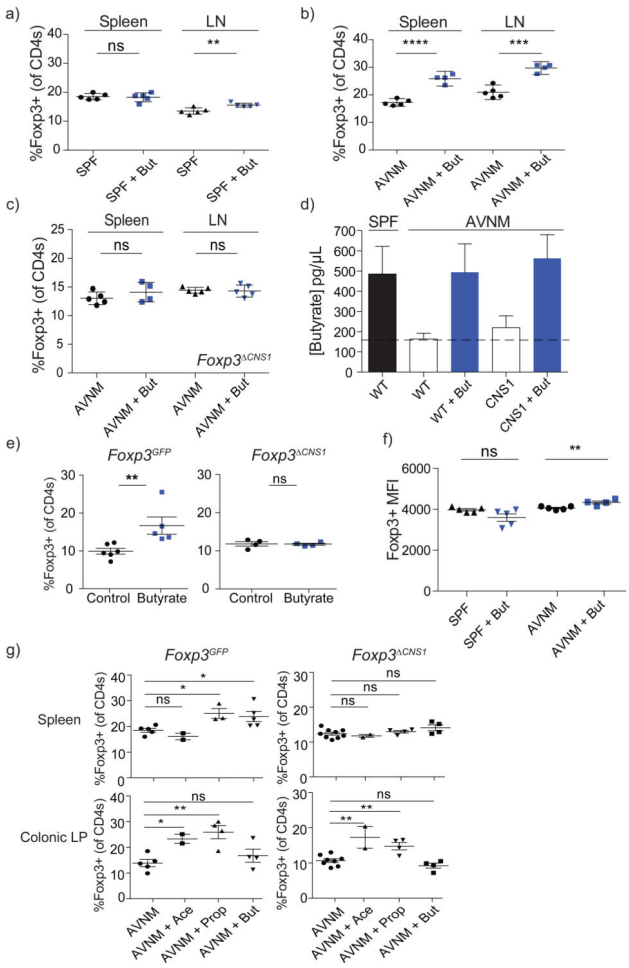

Figure 2. Butyrate provision promotes extrathymic Treg cell generation *in vivo*

a, b) Flow cytometric analysis of Foxp3$^+$ Treg cell subsets in the spleen and lymph nodes (LN) of AVNM-treated (AVNM) or untreated (SPF) B6 or *Foxp3^{GFP}* mice treated with (+But; blue symbols) or without (black symbols) butyrate in drinking water. Data are representative of 3 independent experiments.

c) CNS1-deficient mice were treated with AVNM with or without butyrate as in (a) and analyzed for Foxp3 expression in splenic and lymph node (LN) CD4$^+$ T cell populations. Data are representative of 2 independent experiments.

d) LC-MS analysis of butyrate in serum from CNS1-sufficient B6 (WT) and -deficient mice (CNS1) treated as in (a). Serum was derivatized with 2-nitrophenylhydrazine-HCl. Butyrate levels in serum of untreated (SPF) B6 mice are shown in black. Antibiotic-treated (AVNM) WT and CNS1-deficient animals supplemented with (+But; solid bars) or without (empty bars) butyrate are shown. At least 4 mice per group; error bars denote SEM.

e) Flow cytometric analysis of Foxp3$^+$ Treg cell populations in colonic lamina propria of *Foxp3^{GFP}* (left) and CNS1-deficient mice(right). Mice were administered butyrate (blue symbols) or pH-matched water (control; black symbols) by enema for 7 days and analyzed for Foxp3 expression in colonic CD4$^+$ T cell populations. The data represent the combination of 2 independent experiments; error bars denote SEM.

f) Flow cytometric analysis of Foxp3 protein expression on a per cell basis in splenic Foxp3^{+} Treg cells in B6 mice treated with butyrate (+But) alone (SPF) or in combination with antibiotics (AVNM) as indicated. The data are shown as mean fluorescence intensity (MFI) +/- SD. Data are representative of at least 3 independent experiments.
g) AVNM-treated *Foxp3*^{GFP} (left) and CNS1-deficient mice (right) were administered acetate (Ace), propionate (Prop), butyrate (But), or no SCFA (AVNM) for a period of 3 weeks followed by analysis of Foxp3^{+} Treg cell subsets within CD4^{+} cells isolated from the colonic lamina propria (top panels) or spleens (bottom panels). Data represent the combination of 2 independent experiments; error bars denote SEM.
* $P \leq 0.05$, ** $P \leq 0.01$, *** $P \leq 0.001$, **** $P \leq 0.0001$ as determined by Student's *t*-test.

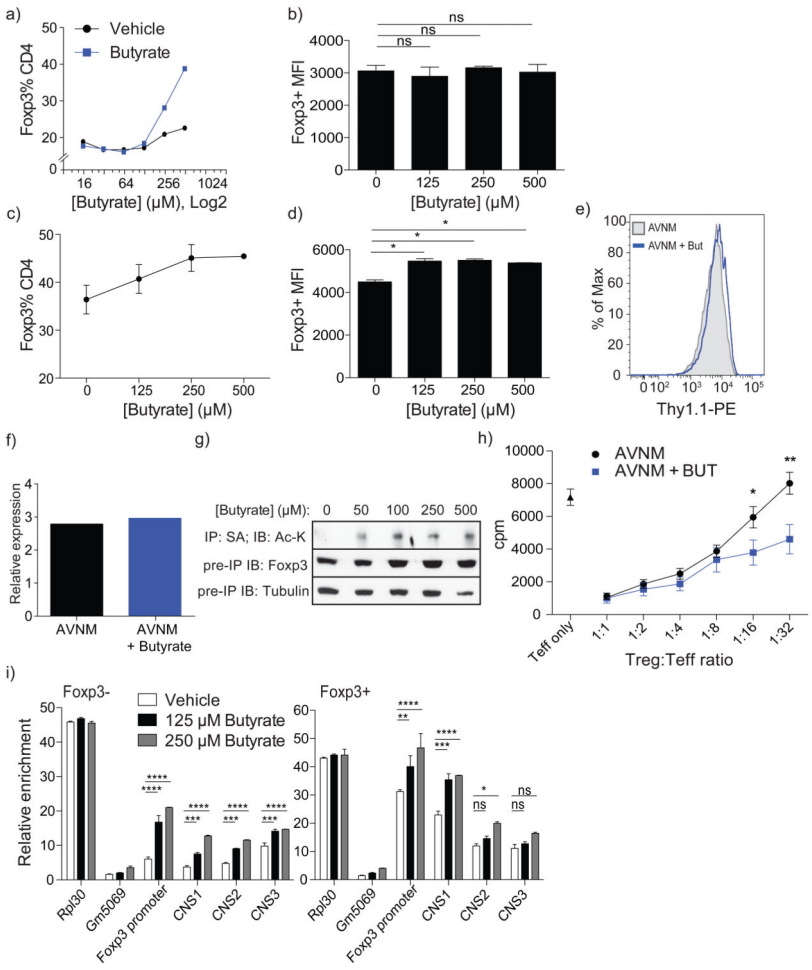

Figure 3. Butyrate acts within T cells to enhance acetylation of the *Foxp3* locus and Foxp3 protein

a) Induction of Foxp3 expression upon stimulation of naïve $CD4^+$ T cells by CD3 antibody in the presence of butyrate-treated or untreated Flt3L-elicited DC and TGF-β. DC were cultured with titrated amounts of butyrate or medium alone for 6 h, washed and co-cultured with FACS-purified naïve $CD4^+$ T cells in the presence of CD3 antibody and TGF-β. The data are shown as percent $CD4^+$ cells expressing Foxp3 after 4 days of culture. Data are representative of at least 4 independent experiments.

b) Analysis of Foxp3 protein expression on a per-cell basis in Treg cells generated in the presence of butyrate pre-treated Flt3L-elicited DC [as in (a)]. The data are shown as mean fluorescence intensity (MFI); error bars denote SEM.

c) Percent of $CD4^+$ cells expressing Foxp3 after 4 days in FACS-sorted naïve $CD4^+$ T cells incubated with CD3/CD28 antibody-coated beads under Treg-inducing conditions. Data are representative of at least 2 independent experiments; error bars denote SEM.

d) MFI of Foxp3 expression in $Foxp3^+$ $CD4^+$ cells from (c). Data are representative of at least 2 independent experiments; error bars denote SEM.

e) Thy1.1 expression in $CD4^+Foxp3^+$ splenocytes isolated from bi-cistronic *Foxp3*$^{Thy1.1}$ reporter mice treated with AVNM with (+But) or without butyrate as described in Figure 2a legend. Cell surface expression of IRES-driven Thy1.1 reporter inserted into the endogenous

Foxp3 locus reflects Foxp3 mRNA levels. The data are representative of at least 3 mice in each group and 2 independent experiments.

f) $CD4^+Foxp3^+$ splenocytes from $Foxp^{GFP}$ reporter mice treated with AVNM with or without butyrate (as in Figure 2a) were FACS-sorted and analyzed for *Foxp3* mRNA expression by qPCR.

g) AVI-tagged Foxp3-expressing TCli hybridoma cells were treated for 15 h with butyrate at the indicated concentrations followed by immunoprecipitation of tagged Foxp3 protein using streptavidin beads and immunoblotting for acetylated-lysine residues (top panel), total Foxp3 protein (middle panel) and tubulin (bottom panel) from pre-precipitation whole cell lysate. Data are representative of 2 independent experiments.

h) Analysis of suppressor capacity of GFP^+ Treg cells sorted from antibiotic-treated (AVNM) $Foxp3^{GFP}$ mice administered (+But) or not administered butyrate in drinking water. Data represent two independent experiments combined with at least 4 mice per group each.

i) FACS-sorted naïve $CD4^+$ T cells isolated from $Foxp3^{GFP}$ animals were incubated with CD3/CD28 antibody-coated beads under Treg-inducing conditions in the presence of indicated amounts of butyrate. $Foxp3^+$ and $Foxp3^-$ $CD4^+$ cells were FACS-purified at day 3 of culture and H3K27 acetylation at the *Foxp3* promoter and CNS1-3 enhancers was assessed using ChIP-qPCR. Enrichment over input for each indicated *Foxp3* regulatory region at given concentrations of butyrate is shown.

Data in this figure are representative of at least 2 independent experiments. The data represent mean +/- SEM. * $P \leq 0.05$, ** $P \leq 0.01$, *** $P \leq 0.001$, **** $P \leq 0.0001$, as determined by Student's *t*-test.

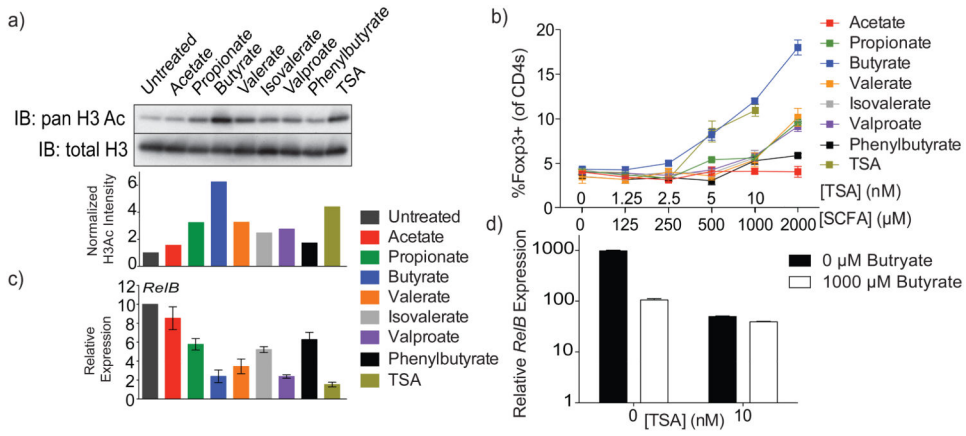

Figure 4. HDAC-inhibitory activity of butyrate decreases pro-inflammatory cytokine expression within DC to promote Treg induction

a) Histone acetylation in Flt3L-elicited DC from B6 mice treated with the indicated SCFA (500 μM) or TSA (10 nM) for 6 h followed by acid extraction of histones from isolated nuclei, SDS-PAGE and blotting with antibody for pan-acetylated H3. Total histone H3 served as a loading control. Shown below is the relative acetylated H3 band intensity calculated over total H3 and normalized as fold over untreated.

b) Induction of Foxp3 expression upon stimulation of naïve $CD4^+$ T cells by CD3 antibody in the presence of SCFA or TSA, Flt3L-elicited DC and TGF-β. DC were cultured with titrated amounts SCFA or TSA for 6 h, washed and co-cultured with FACS-purified naïve $CD4^+$ T cells in the presence of CD3 antibody and TGF-β. The data are shown as percent $CD4^+$ cells expressing Foxp3 after 4 days of culture. Data are representative of at least 2 independent experiments.

c) *RelB* gene expression quantified by qPCR in purified Flt3L-elicited DC from B6 mice treated for 6 h with SCFA or TSA, as in (a). Data are representative of 4 independent experiments.

d) *RelB* gene expression quantified by qPCR in purified Flt3L-elicited DC from B6 mice treated with or without TSA in combination with, or in the absence of, butyrate at the indicated concentrations.

Data in this figure are representative of at least 2 independent experiments, unless otherwise noted. The data represent mean +/- SEM.